16

Role of multipole interaction to the appearance of the red-shifted Mi-Frohlich resonance induced by an interacting pairs of copper nanoparticles encapsulated by an amorphous carbon matrix

© I.E. Istomin, S.G. Yastrebov¶, T.N. Vasilevskaya

Ioffe Institute,
St. Petersburg, Russia

¶ E-mail: yastrebov@mail.ioffe.ru

Received February 21, 2025
Revised February 22, 2025
Accepted February 24, 2025

A model that takes into account the contribution to optical absorption of the interaction between neighboring copper nanoclusters forming dimers is proposed. It allows to explain the splitting of the Mi-Frelich resonance experimentally observed in layers of amorphous hydrogenated carbon modified with copper. The model also predicts quite accurately the absolute values of the resonance frequencies observed experimentally.

Keywords: plasmonics, metal nanoparticles, dimers.

DOI: 10.61011/PSS.2025.02.60693.38-25

1. Introduction

Optical properties of amorphous carbon, also known as diamond-like carbon, are easily modulated by metal additives, thus, causing alteration of optical properties by surface plasma resonances localized in metal nanoparticles, for example, copper [1–4]. These resonances are also known as the Mie-Frohlich (MF) resonances [4]. Metals may be added by various techniques. Thus, combined magnetron sputtering of carbon and copper targets may be used to produce a carbon-copper nanocomposite [1]. More recently, it was found experimentally that MF resonance band was split into two lognormal loops, low-frequency and high-frequency, respectively [4], with maximum positions 1.6 eV and 1.8 eV.

The effect of electrostatic dipole interactions on the MF resonance behavior in approach of copper clusters was discussed in [4]. It was shown that the resonance frequency shift varies multidirectionally depending on the electric field orientation with respect to dimer axis.

However, in [4] positions of both peaks 1.8 eV and 1.6 eV couldn't be explained by varying the distance between the cluster edges and field direction on the assumption that the dielectric function of copper is independent on the cluster dimer. This study investigates the effect of multipole moments from the distance between spherical copper clusters that form dimers. It will be shown that the consideration of contribution to absorption by excitation of multipole and dipole modes, interacting copper nanoparticles combined into a dimer explains the nature and position of both peaks ~ 1.6 and ~ 1.8 eV. Applied significance of the findings of this work is very important because they may be used in engineering of nano-composites capable of absorbing IR and RF electromagnetic radiation. The findings may be also used for interpreting optical properties of hybrids of new allotropic forms of carbon such as graphene layers modified with copper nanoparticles such as produced in [5].

2. Experiment

Experimental details are given in [4]. Note here that analysis of the image of a nano-composite structure based on copper-modified amorphous copper was carried out in [4]. It was determined that particles have a near-spherical shape. Statistical analysis of particle distribution over diameters and distances between nanoparticle edges was performed.

It was found that the median diameter of nanoparticles $D = 2$ nm, and the median distance between the nearest particle edges was also equal to 2 nm. Optical spectroscopy and further processing of spectra were used to determine that the absorption spectrum of a nano-composite produced with an area ratio of copper and graphite targets of 0.12 can be decomposed into two lognornal curves with maxima ~ 1.6 eV and ~ 1.8 eV

3. Model and results

We consider a pair of copper nanoparticles in an amorphous carbon matrix. Permittivity of amorphous carbon having low dispersion in the given frequency range is assumed as constant and equal to 5.02 (according to [4]). Dielectric copper function was calculated as described in [4]. As mentioned above, the particle surface shape will be assumed as spherical. Schematic diagram of the system consisting of two spheres is shown in Figure 1, *a*.

Two nanoparticles are interconnected by induced electric fields. Consider the extinction cross-section of a pair of particles shown in Figure 1. As the size of the pair

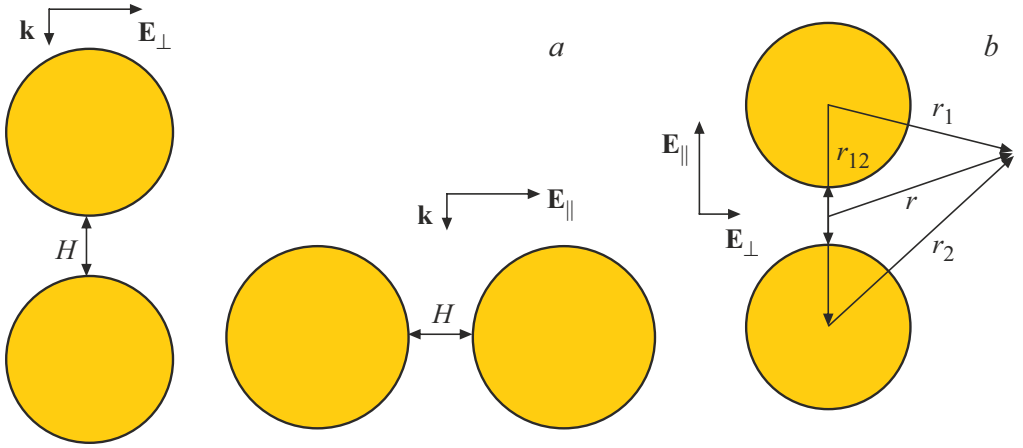

Figure 1. *a*) Schematic diagram of a cluster consisting of two spherical nanoparticles. The first diagram is an electric field of an electromagnetic wave falling on particles parallel to the straight line connecting the centers of spheres. The second diagram is an electric field of an electromagnetic wave falling on particles perpendicularly to the straight line connecting the centers of spheres. *b*) Diagram indicating the quantities used in the calculation.

of particles is small compared with the electromagnetic wave length, electrostatic approximation may be used for calculation. Figure 1, *b* shows a scheme that explains the parameters used for calculation. To find electrical fields induced by nanoparticles in a random point shown in Figure 1, *b* as a bullet, the Laplace equation for potential (ψ) is used [6,7]:

$$\Delta\psi = 0. \tag{1a}$$

To solve this equation, boundary conditions are specified for each sphere [6,7]:

$$\begin{aligned}
\psi\big|_{R_1+0} &= \psi|_{R_1-0}, \\
\psi\big|_{R_2+0} &= \psi\big|_{R_2-0}, \\
\varepsilon_m \frac{\partial\psi}{\partial r}\bigg|_{R_1+0} &= \varepsilon \frac{\partial\psi}{\partial r}\bigg|_{R_1-0}, \\
\varepsilon_m \frac{\partial\psi}{\partial r}\bigg|_{R_2+0} &= \varepsilon \frac{\partial\psi}{\partial r}\bigg|_{R_2-0},
\end{aligned} \tag{1b}$$

where
$R_1 + 0$ — denotes the outer boundary of sphere 1;
$R_2 + 0$ — denotes the outer boundary of sphere 2;
$R_1 - 0$ — denotes the inner boundary of sphere 1;
$R_1 - 0$ — denotes the inner boundary of sphere 2;
r — vector radius-module ; ε and ε_m are permittivities of copper and amorphous carbon, respectively.

Solution of equation (1a) outside the spheres may be represented as a sum of two solutions for each of the spheres $\psi = \psi_1^{out} + \psi_2^{out}$ (ψ_1 is the potential induced by sphere 1, ψ_2 is the potential induced by sphere 2). For each ψ_1^{out} and ψ_2^{out}, the Laplace equation is also valid:

$$\Delta\psi_1^{out} = 0, \quad \Delta\psi_2^{out} = 0. \tag{1c}$$

Solution of equation (1a) inside spheres 1 and 2 in a spherical coordinate system will be, respectively, written as:

$$\begin{aligned}
\psi_1^{in} &= \sum_{l=0}^{\infty}\sum_{m=-l}^{l} b_{lm}^{(1)} r_1^l Y_{lm}(\theta_1, \varphi_1), \\
\psi_2^{in} &= \sum_{l=0}^{\infty}\sum_{m=-l}^{l} b_{lm}^{(2)} r_2^l Y_{lm}(\theta_2, \psi_2),
\end{aligned} \tag{2a}$$

where $b_{lm}^{(1)}$, $b_{lm}^{(2)}$ are the coefficients corresponding to sphere 1 and 2, $Y_{lm}(\theta, \varphi)$ are spherical harmonics. Solution of equations (1c) in a spherical coordinate systems will be written as:

$$\begin{aligned}
\psi_1^{out} &= \sum_{l=0}^{\infty}\sum_{m=-l}^{l} a_{lm}^{(1)} r_1^{-l-1} Y_{lm}(\theta_1, \varphi_1), \\
\psi_2^{out} &= \sum_{l=0}^{\infty}\sum_{m=-l}^{l} a_{lm}^{(2)} r_2^{-l-1} Y_{lm}(\theta_2, \psi_2),
\end{aligned} \tag{2b}$$

where $a_{lm}^{(1)}$, $a_{lm}^{(2)}$ are the coefficients corresponding to sphere 1 and 2. Then boundary conditions (1b) will be written as:

$$\begin{aligned}
(\psi_1^{out} + \psi_2^{out} + \psi_0)\big|_{R_1} &= \psi_1^{in}\big|_{R_1}, \\
(\psi_1^{out} + \psi_2^{out} + \psi_0)\big|_{R_2} &= \psi_2^{in}\big|_{R_2}, \\
\varepsilon_m \frac{\partial(\psi_1^{out} + \psi_2^{out} + \psi_0)}{\partial r}\bigg|_{R_1} &= \varepsilon \frac{\partial\psi_1^{in}}{\partial r}\bigg|_{R_1}, \\
\varepsilon_m \frac{\partial(\psi_1^{out} + \psi_2^{out} + \psi_0)}{\partial r}\bigg|_{R_2} &= \varepsilon \frac{\partial\psi_2^{in}}{\partial r}\bigg|_{R_2},
\end{aligned} \tag{2c}$$

where $\psi_0 = a_{10}^{(0)} Y_{10}(\theta, \varphi)$ is the external field potential. By substituting solutions (2a) and (2b) into the boundary

conditions (2c), a system of equations for $a_{lm}^{(1)}$, $a_{lm}^{(2)}$ is obtained, $b_{lm}^{(1)}$, $b_{lm}^{(2)}$ [6,7]:

$$\begin{cases} a_{lm}^{(1)} + \sum\limits_{l'=0}^{\infty} \sum\limits_{m'=-l'}^{l'} \alpha_l C_{l',l}^{m',m} T_{l'+l}^{m'-m}(\mathbf{r}_{12}) a_{l'm'}^{(2)} = -\alpha_l a_{lm}^{(0)}, \\ a_{lm}^{(2)} + \sum\limits_{l'=0}^{\infty} \sum\limits_{m'=-l'}^{l'} \alpha_l C_{l',l}^{m',m} T_{l'+l}^{m'-m}(\mathbf{r}_{21}) a_{l'm'}^{(1)} = -\alpha_l a_{lm}^{(0)}, \\ b_{lm}^{(1)} + \dfrac{a_{lm}^{(1)}}{R^{2l+1}} \sum\limits_{l'=0}^{\infty} \sum\limits_{m'=-l'}^{l'} C_{l',l}^{m',m} T_{l'+l}^{m'-m}(\mathbf{r}_{12}) a_{l'm'}^{(2)} + a_{lm}^{(0)}, \\ b_{lm}^{(2)} + \dfrac{a_{lm}^{(2)}}{R^{2l+1}} \sum\limits_{l'=0}^{\infty} \sum\limits_{m'=-l'}^{l'} C_{l',l}^{m',m} T_{l'+l}^{m'-m}(\mathbf{r}_{21}) a_{l'm'}^{(1)} + a_{lm}^{(0)}, \end{cases} \tag{3a}$$

where R — sphere radius,

$$\alpha_l = R^{2l+1} \frac{(\varepsilon - \varepsilon_m)}{\left(\varepsilon + \frac{l+1}{l}\varepsilon_m\right)},$$

$$C_{l',l}^{m',m} =$$

$$= \sqrt{\frac{4\pi}{2(l+l')+2} \frac{(l+l'+m-m')!}{(l+l'-m+m')!} \frac{2l+1}{2l'+1} \frac{(l'+m')!}{(l+m)!} \frac{(l-m)!}{(l'-m')!}}$$

$$\times \frac{(-1)^{\left(l+\frac{(|m|+|m'|-|m-m'|)}{2}\right)} (l+l'-|m-m'|)!}{(l-|m|)!(l'-|m'|)!},$$

$$T_l^m(\mathbf{r}) = \frac{Y_l^m(\theta,\varphi)}{r^{l+1}}, \quad a_{lm}^{(0)} = -\sqrt{\frac{4\pi}{3}} E_0 \delta_{l1} \delta_{m0},$$

δ_{ij} — Kronecker symbol. E_0 — electric field strength of an incident electromagnetic wave, assume $E_0 = 1$.

To find the scattering cross-section in the „forward scattering“ configuration, multipole moments shall be linked to $a_{lm}^{(1)}$ and $a_{lm}^{(2)}$ [6]:

$$Q_{lm}^{(1,2)} = a_{lm}^{(1,2)} \sqrt{\frac{2l+1}{4\pi}},$$

$$Q_{lm} = Q_{lm}^{(1)} + Q_{lm}^{(2)}. \tag{4}$$

Scattering cross-section C_{sca} and extinction cross-section C_{ext} are calculated through multipoles (4) as follows, respectively [6,7]:

$$C_{sca} = 4\pi \sum_{0}^{\infty} \sum_{m=-l}^{l} k^{2l+2} \frac{(l+1)(2l+1)}{l\left((2l+1)!!\right)^2} |Q_{lm}|^2,$$

$$C_{ext} = 4\pi \sum_{0}^{\infty} \sum_{m=-l}^{l} \mathrm{Re}\left(\frac{(-i)^{l+1} k^l}{(2l+1)!!l} \sqrt{\frac{(l+1)(2l+1)}{(l+1)}} \right.$$

$$\left. \times Q_{lm} \frac{\partial Y_{lm}(\theta,\varphi)}{\partial\theta}\bigg|_{\substack{\theta=\pi/2,\\ \varphi=0}} \right), \tag{5}$$

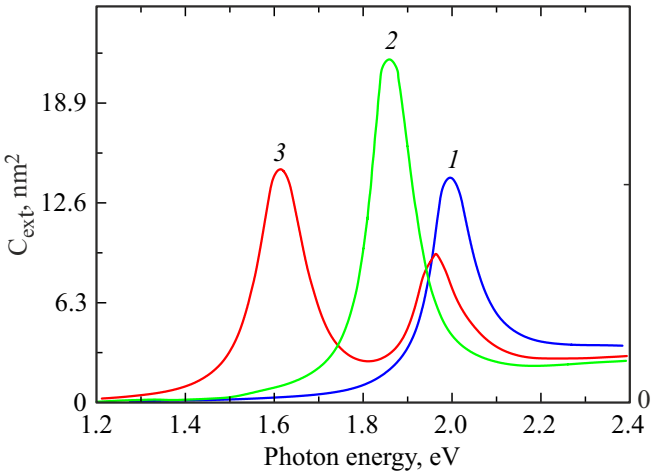

Figure 2. Extinction cross-section for the parallel field orientation and the interparticle distance $H = 1.5$ Å, $D = 2$ nm. The blue curve (*1*) shows the extinction cross-section for a pair of noninteracting particles, the green curve (*2*) shows the extinction cross-section for a pair of particles with dipole-dipole interaction, the red curve (*3*) shows the extinction cross-section for a pair of particles with multipole interaction.

where **k** is the wave number, corresponding angles are equal to those for the spherical coordinate system.

For calculation, infinite sums in equations (3a) and (5) are replaced with finite sums with the number of elements $l = 16$ (number of multipoles). Note that number 16 is chosen from consideration that the variation of maximum extinction coefficient position is small as the number of multipoles per unit increases.

The calculation results using equation (5) are shown in Figure 2. The same figure shows the calculation of interacting dipoles excited in the neighboring nanoparticles, which corresponds to the $l = 1$ case (dipole interaction). The calculation showed that the scattering cross-section is much lower than the extinction cross-section. Therefore, Figure 2 shows a spectral dependence of the extinction cross-section. The extinction and scattering coefficients of noninteracting particles are calculated using expressions [7]:

$$C_{ext} = 4\pi k \varepsilon_m^{1/2} \mathrm{Re}(i\alpha),$$

$$C_{scat} = 8/3\pi \left(\varepsilon_m^{1/2} k\right)^4 |\alpha|^2,$$

$$\alpha = \frac{\varepsilon - \varepsilon_m}{\varepsilon + 2\varepsilon_m} R^3. \tag{6}$$

Blue curve in Figure 2 (curve *1*) shows the extinction cross-section, because the scattering cross-section in the given case turned to be negligibly small throughout the frequency range. Figure 2 shows that MF resonance with frequency ~ 2 eV corresponds to single noninteracting particles. To consider the interaction, such parameter as the distance between nanoparticle edges, H shall be used. It was determined by calculation that the best agreement with the experiment is achieved when $H = 0.15$ nm. It follows

from the green dependence on frequency (curve *2*) that the consideration of dipole interaction between particles leads to a red resonance shift from ~ 2 to ~ 1.84 eV. This value is close to the experimental peak 1.8 eV [4]. Red dependence on frequency (curve *3*) in turn shows that, when multipoles are considered, the MF resonance frequency is split into two frequencies, the low-frequency resonance shifts to ~ 1.6 eV, and the high-frequency resonance, as in the noninteracting particles case, appears at the frequency of ~ 2 eV.

Note that an identical calculation performed for the electric field orientation perpendicular to the axis didn't give a resonance shift towards the low-frequency spectrum region.

Thus, the description of absorption spectrum of the amorphous carbon and copper nano-composite using the spherical particle model shall consider the presence of dimers, whose components are covered by dipole interaction, in order to explain the absorption peak with a maximum about 1.84 eV. To explain the peak with a maximum of 1.6 eV, contribution to absorption made by adjacent pairs of copper nanoclusters covered by the multipole interaction shall be considered.

4. Conclusion

Consideration of the dipole and multipole interaction between the spherical particles, which are immersed into the amorphous carbon and grouped in dimers, explains the appearance of the MF resonance with frequencies of ~ 1.8 and ~ 1.6 eV.

Conflict of interest

The authors declare no conflict of interest.

References

[1] T.N. Vasilevskaya, S.G. Yastrebov, N.S. Andreev, I.A. Drozdova, T.K. Zvonareva, V.N. Filippovich. FTT **41**, *11*, 2088 (1999). (in Russian).
[2] I. Yaremchuk, Š. Meškinis, T. Bulavinets, A. Vasiliauskas, M. Andrulevičius, V. Fitio, Ya. Bobitski, S. Tamulevičius. Diam. Relat. Mater., **99**, 107538 (2019). https://doi.org/10.1016/j.diamond.2019.107538.
[3] S. Tamulevičius, Š. Meškinis, T. Tamulevičius, H.G. Rubahn. Rep. Prog. Phys. **81**, *2*, 024501 (2018). https://doi.org/10.1088/1361-6633/aa966f
[4] I. Istomin, S. Yastrebov, M.R. Singh. Diam. Relat. Mater. **136**, 109962 (2023). https://doi.org/10.1016/j.diamond.2023.109962.
[5] I.D. Bernardo, J. Bradford, Z. Fusco, J. Mendoza, T. Tran-Phu, R. Bo, N. Motta, A. Tricolia. J. Mater. Chem. C, **8**, 11896 (2020). https://doi.org/10.1016/10.1039/D0TC02848G
[6] J.D. Jackson. *Classical Electrodynamics* (New York, Wiley, 1999).
[7] C.F. Bohren, D.R. Huffman. *Absorption and Scattering of Light by Small Particles* (New York,Wiley, 1983).

Translated by E.Ilinskaya